IEEE Access
Multidisciplinary | Rapid Review | Open Access Journal

Received December 4, 2020, accepted December 17, 2020, date of publication December 22, 2020,
date of current version December 31, 2020.

*Digital Object Identifier 10.1109/ACCESS.2020.3046635*

# A New Alignment and Breakthrough Accuracy Optimization Strategy in Long Immersed Tunnel Surveys

**GUANQING LI[1], SHENGXIANG HUANG[1], XINPENG WANG[2], CHENFENG LI[1], AND WEN ZHANG[1]**

[1]School of Geodesy and Geomatics, Wuhan University, Wuhan 430079, China
[2]Department of Surveying and Mapping Engineering, College of Mining, Guizhou University, Guizhou 550025, China

Corresponding author: Shengxiang Huang (shengxhuang@163.com)

This work was supported in part by China Scholarship Council (CSC) under Grant 201906270175.

**ABSTRACT** For ultra-long tunnels, the effective means of alignment and breakthrough accuracy optimization is to measure the gyro azimuths or transfer the coordinates of surface known points or the directions to the inside of the tunnel through vertical shafts or inclined shafts. Compared with bored tunnels, immersed tunnels have different engineering characteristics and construction environments, and have higher alignment control accuracy requirements. However, the immersed tunnel has no vertical shafts or inclined shafts that can be used for coordinate transfer to improve the measurement accuracy. In order to provide high-accuracy alignment control and breakthrough for long immersed tunnels, we put forward a new strategy after network stability analysis, and consistency analysis between the results of the element positioning system and the results of the control network. The results of the element positioning system are taken as constraints to improve the accuracy of the control network. The analysis on 100,000 simulations of a 20 km-long immersed tunnel shows that the accuracy of the last point pair of the traverse network with angle and distance observations is 60.8 mm, while the accuracy of the same point pair after adopting the new strategy in this paper is 11.8 mm. The results of a 7 km-long experimental traverse network show that the lateral breakthrough accuracy is improved by 73%. All of these indicate that the new strategy can effectively improve the measurement accuracy and the lateral errors can be kept at a small level. Following the new strategy, the high-accuracy alignment and breakthrough can be achieved for long immersed tunnels.

**INDEX TERMS** Alignment control, breakthrough accuracy, immersed tunnel, joint adjustment, positioning system, traverse network.

## I. INTRODUCTION

Ensuring the accurate meeting of the tunnels constructed from two opposite directions is a very important task in tunnel engineering surveys. However, it was from the Channel Tunnel that links Britain and France, and some other long tunnels, that the alignment errors and their estimation began to receive attention [1]–[6]. Comprehensive mathematical analysis should be carried out in advance to determine the appropriate control network configuration and the observation scheme. A surface network and an underground network are usually established for tunneling surveys. The surface network covers the tunnel area to control the whole project. The Global Navigation Satellite Systems (GNSS) and terrestrial techniques can be used to provide the coordinates near the portals. The underground network controls the construction procedure.

Due to the absence of the satellite signals and the narrow space, it is a challenge to carry out the high-accuracy coordinate transfer inside the tunnel. Firstly, the flexibility of the inside network layout is not great. It is impossible to choose a network with ideal geometry like the surface control network. Moreover, the effect of refraction on optical measurements caused by the variation of temperature and the air pressure is a major source of errors [7]. In theory, the refraction index is assumed to be constant along the tunnel axis and its variation pattern has the axial symmetry, so the traverse along the tunnel axis is the most suitable geometry to reduce the effect [2], [3], [8]. But the tunnel axis needs to be kept free most of time. In reality, a *zigzag* traverse is usually designed to

The associate editor coordinating the review of this manuscript and approving it for publication was Di He.

minimize the lateral refraction effect [7], [9], [10]. If the tunnel is curved, a *zigzag* traverse is less effective at reducing the effects of lateral refraction, and a double *zigzag* can be run [3], [11]

In addition, the refraction index can be measured with a scintillometer to calculate the corrections for the line of sight curvature. Or the refraction-free measurements can be collected using dispersometers. However, due to the complexity of related measurement procedures, methods for determining or correcting the refractive effects are not widely adopted [12].

The use of gyrotheodolites can verify the quality of the angle and distance observations, and improve the accuracy of the traverse. It is confirmed that the refractive effect can be significantly decreased by measuring the gyro azimuths [2], [13]. The gyrotheodolite's application in tunnels has been discussed in many literatures, such as [5], [7], [9], [14]. Martusewicz studied the optimal location of the extra gyroscopic azimuth in underground traverse [15]. Strategies for gyro data processing have also been improved. The network adjustment with fixed gyro observations, with equally weighted gyro azimuths, and with self-adaptive weighted gyro azimuths were gradually proposed [16], [17].

Increasing the complexity of the network is another solution to improve the accuracy and reliability of the network inside the tunnel. For example, the duo-linear joint chain was designed for the Hong Kong-Zhuhai-Macau immersed tunnel construction. Compared with the traverse, the chain consists of four points per point pair and has more redundant observations [18], [19]. Besides, free station setup can be established and additional observations can be made between wall points [20]. When the tunnel is very long, the known coordinates or azimuths can be transfered by the access tunnel or shaft. This method of improving precision has been proved to be very effective in long tunnel [9], [21].

The immersed tunnel is composed of prefabricated elements. For good water tightness, each element needs to be accurately connected to the previous one. Compared with the bored tunnels, the immersed tunnel has higher alignment control and breakthrough accuracy requirements. Taking Hong Kong-Zhuhai-Macau immersed tunnel as an example, its length is 6.7 km, and the breakthrough accuracy is required to be $\pm 35$ mm. According to the current Chinese specifications, the breakthrough error of tunnels of the same length shall not be greater than $\pm 75$ mm. The longest immersed tunnel planned in the world is 17 km [22]. It is very difficult to meet the accuracy requirements of the immersed tunnel by relying on the present strategy of tunneling surveys.

According to the construction characteristics of the immersed tunnel, a new strategy for alignment control and breakthrough accuracy optimization in long immersed tunnel is proposed in this paper. During the element installation process, a positioning system is used to provide the position and attitude angles of the element in real time (Fig. 1). The commonly used element positioning system is the measurement tower system, which consists of two measurement towers.

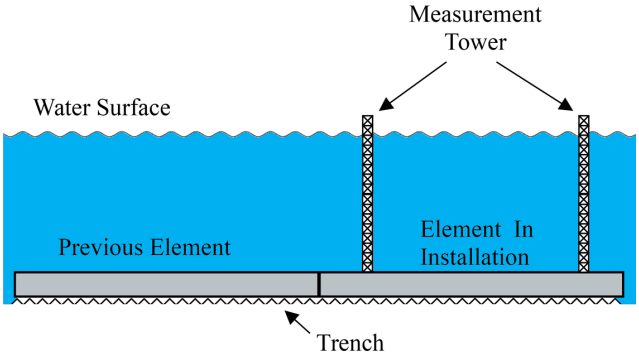


**FIGURE 1.** The element positioning system of the immersed tunnel. The position of the element in installation can be obtained by measuring the coordinates of the top of the towers.

The measurement tower is always above the water during the installation of the element. By measuring the coordinates of the points on the top of the tower, the position and attitude angles of the element can be calculated. After the element installation is finished, the positioning system provides the ''final'' position of the element. The inside breakthrough survey is performed to get the ''accurate'' position of the element. The ''accurate'' position is used to check the ''final'' position, to confirm the current position, and to see whether it is necessary to accurately adjust the position of the element. The alignment control of the tunnel is subject to the breakthrough survey results. The real-time lateral accuracy requirement of the element position is less than 50 mm, and the accuracy of the positioning system is generally better than 30 mm [23]. Hence, after certain analysis, we take the ''final'' position as the constraints and perform the adjustment together with the inside control network to improve the accuracy of the alignment control of the immersed tunnel.

The paper is organized as such: the present alignment control strategy is described in Section II; Section III gives the method of stability analysis of the element and illustrates the stability of the points inside the immersed tunnel with an example; the new strategy is described in detail in Section IV; in Section V, the performance of the new strategy is illustrated by simulations and an experiment; the conclusions are given in Section VI.

## II. PRESENT ALIGNMENT AND BREAKTHROUGH ACCURACY OPTIMIZATION STRATEGY

### A. OPTIMIZATION OF ALIGNMENT AND BREAKTHROUGH ACCURACY

There are four different orders of optimizing a control network [24]. In addition to improving the accuracy of observations, the optimization of the breakthrough accuracy is usually carried out from two perspectives, namely, control network design and adding observation types. According to the different lengths of the tunnels and the breakthrough accuracy requirements, the control network can be run as a *zigzag* traverse, a double *zigzag* traverse (Fig. 1a), a double traverse with common stations or a traverse network (Fig. 1b), or a duo-linear joint chain (Fig. 1c). The more complex the

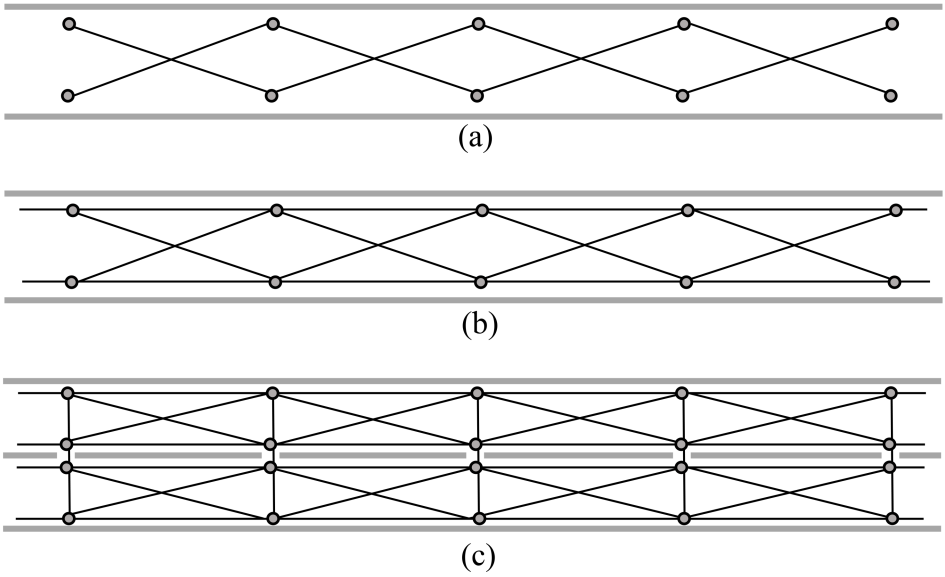


**FIGURE 2.** The different configurations of control network in the tunnels. (a) double *zigzag* traverse, (b) double traverse with common stations, (c) duo-linear joint chain.

graphic structure of the control network, the more redundant observations, the smaller the amplitude of the control network's left-right swing under the influence of the angle errors, and the higher the accuracy of the control network when the accuracy of the observations is the same. Based on the compromise between the visibility conditions and the accuracy requirements, the optimal side length should be determined by means of simulations. For example, after analysis, Velasco found a side length of 375 m was the optimum distance for a 25 km tunnel in Spain [9], while Huang chose a side length of 720 m for the longest immersed tunnel ever built in the world [18].

For ultra-long tunnels, the accuracy of breakthrough depends largely on the additional azimuth observations. The azimuth angle can be measured with a gyrotheodolite or transferred through a shaft from the surface. Such observations are absolute azimuths, unaffected by the propagation of angle errors. Azimuth observations can not only improve the accuracy, but also carry out an independent check of the control network. For example, the 57.5 km Gotthard Base Tunnel has several intermediate tunnels, vertical shafts, exploring tunnels, and bypasses. For the intermediate attack at Sedrun, the direction was transfered from the surface (1340 m) to the tunnel level (540 m) through a vertical shaft with a diameter of 8 m. In addition to the gyrotheodolite, precise plumbing with the dispersometer using mercury plumbing instruments, polarised dual-wavelengths light, and inertial systems were also used to transfer the azimuths. Finally, the requirements of 100 mm breakthrough error were met at all breakthrough surfaces [13]. According to the consequence of the simulations carried out in [9], the use of a gyrotheodolite is considered to be mandatory for tunnels longer than 15 km.

With the extension of the tunnel, new control points are continuously laid forward. Generally the control network needs to be measured at regular intervals. Each survey starts from the surface known points. The observations will be processed in the method described in the following subsection to produce the coordinates for further setting out in the tunnel, and to check the displacement of the underground points.

### B. DATA PROCESSING

Observations of the control network inside the immersed tunnel include angles $L_\theta$ and distances $L_s$, and sometimes azimuths $L_a$. The steps of data processing include the outlier detection, the variance component estimation (VCE) and the constraint adjustment [18]. $L_\theta$, $L_s$ and $L_a$ are independent. The angles and azimuths are assumed to be of equal accuracy. Their accuracy is $\sigma_\theta$ and $\sigma_a$, respectively. The accuracy of the distance is related to its length and is expressed as $\sigma_{s_i} = \sigma_s(1 + c \times s_i)$. $c$ is equal to $b/a$ and is assumed to be fixed. $a$ and $b$ are the fixed and proportional errors of the distance measurement.

According to the observation types, the observation equations are:

$$\begin{cases} v_\theta = A_\theta \hat{x} - l_\theta \\ v_s = A_s \hat{x} - l_s \\ v_a = A_a \hat{x} - l_a, \end{cases} \tag{1}$$

where $v_*$, $A_*$ and $l_*$ are the residual vector, the design matrix and the constant vector of measurements corresponding to the category of the observation; $\hat{x}$ is the parameter estimations. The cofactor matrix $Q$ is

$$Q = \begin{bmatrix} Q_\theta & 0 & 0 \\ 0 & Q_s & 0 \\ 0 & 0 & Q_a \end{bmatrix} = \begin{bmatrix} \sigma_\theta^2 U_\theta & 0 & 0 \\ 0 & \sigma_s^2 U_s & 0 \\ 0 & 0 & \sigma_a^2 U_a \end{bmatrix} \tag{2}$$

where $U_\theta = I_{n_1}$, $U_s = diag[(1 + cs_1)^2, \ldots, (1 + cs_{n_2})^2]$, $U_a = I_{n_3}$. $n_1, n_2$ and $n_3$ are the number of the angles, distances and azimuths.

To detect the outlier for the $i^{th}$ measurement, the test statistic can be constructed as [25], [26]

$$W_i = \frac{c_i^T P Q_{vv} P l}{\sigma_0 \sqrt{c_i^T P Q_{vv} P c_i}} \tag{3}$$

$c_i = [0, \ldots, 0, 1, 0, \ldots, 0]$ with all elements of 0 except the $i^{th}$ element of 1. $P$ is the weight matrix. $P = Q^{-1}$. $l = (l_\theta^T, l_s^T, l_a^T)^T$. $Q_{vv}$ is the cofactor matrix of the estimated residuals. $Q_{vv} = Q - A(A^T P A)^{-1} A^T$. For an observation, if

$$|w_i| > c_\alpha = N_{1-\alpha/2} \tag{4}$$

the observation is considered to be outlier. $N_{1-\alpha/2}$ is the lower percentage point of a standard normal distribution and $\alpha$ is the level of significance of test.

To achieve the optimal estimates and obtain the correct and realistic posteriori accuracy for the parameters, the correct stochastic model should be applied [27], [28]. If the smaller prior observation accuracy is incorrectly used, the derived coordinate accuracy would be too optimistic [29]. For the immersed tunnel that requires high alignment control accuracy, accepting falsely high-accuracy measurement results can lead to major accidents.

VCE is applied to find the realistic and reliable variance components of the observations to construct the covariance matrix correctly. The Helmert type of VCE reads [30]

$$\begin{bmatrix} H_\theta & H_1 & H_2 \\ H_1 & H_s & H_3 \\ H_2 & H_3 & H_\alpha \end{bmatrix} \cdot \begin{bmatrix} \hat{\sigma}_{\theta,0}^2 \\ \hat{\sigma}_{s,0}^2 \\ \hat{\sigma}_{\alpha,0}^2 \end{bmatrix} = \begin{bmatrix} v_\theta^T Q_\theta^{-1} v_\theta \\ v_s^T Q_s^{-1} v_s \\ v_\alpha^T Q_\alpha^{-1} v_\alpha \end{bmatrix} \tag{5}$$

$$\begin{cases} H_\theta = n_1 - 2tr\left(N^{-1} N_\theta\right) + tr\left(N^{-1} N_\theta\right)^2 \\ H_s = n_2 - 2tr\left(N^{-1} N_s\right) + tr\left(N^{-1} N_s\right)^2 \\ H_\alpha = n_3 - 2tr\left(N^{-1} N_\alpha\right) + tr\left(N^{-1} N_\alpha\right)^2 \\ H_1 = tr\left(N^{-1} N_\theta N^{-1} N_s\right) \\ H_2 = tr\left(N^{-1} N_\theta N^{-1} N_\alpha\right) \\ H_3 = tr\left(N^{-1} N_s N^{-1} N_\alpha\right) \end{cases} \tag{6}$$

$tr(*)$ is the operator to compute the trace of a matrix.

$$\begin{cases} N_\theta = \dfrac{A_\theta^T A_\theta}{\sigma_{\theta,0}^2} \\ N_s = \dfrac{A_s^T U_s^{-1} A_s}{\sigma_{s,0}^2} \\ N_\alpha = \dfrac{A_\alpha^T A_\alpha}{\sigma_{\alpha,0}^2} \end{cases} \tag{7}$$

$$N = N_\theta + N_s + N_\alpha \tag{8}$$

where $\sigma_{\theta,0}^2$, $\sigma_{s,0}^2$, and $\sigma_{\alpha,0}^2$ are the approximate angle, distance and azimuth variances, and will be updated in iterations until $\sigma_{\theta,0}^2 \approx \sigma_{s,0}^2 \approx \sigma_{\alpha,0}^2$. The simplified VCE formulas are:

$$\hat{\sigma}_\theta^2 = \frac{v_\theta^T v_\theta}{n_1 - tr(N^{-1} N_\theta)} \tag{9}$$

$$\hat{\sigma}_s^2 = \frac{v_s^T U_s^{-1} v_s}{n_2 - tr(N^{-1} N_s)} \tag{10}$$

$$\hat{\sigma}_\alpha^2 = \frac{v_\alpha^T v_\alpha}{n_3 - tr(N^{-1} N_\alpha)} \tag{11}$$

Outlier detection and VCE are performed alternately. The clear observations and realistic stochastic model will be acquired. The coordinate estimations of the inside network points are

$$\hat{x} = N^{-1} A^T Q^{-1} l \tag{12}$$

where the design matrix $A$ is:

$$A = \begin{bmatrix} A_\theta \\ A_s \\ A_\alpha \end{bmatrix} \tag{13}$$

Its covariance matrix is

$$D_{\hat{x}\hat{x}} = \frac{v^T Q^{-1} v}{r} (A^T Q^{-1} A)^{-1} \tag{14}$$

where $r$ is the number of redundant observation. $v = (v_\theta^T, v_s^T, v_\alpha^T)^T$.

## III. STABILITY ANALYSIS

The premise of the new alignment and breakthrough accuracy optimization strategy is that (part of) the underground points are stable, so the stability analysis of the network points is first required. Many researchers have conducted extensive research on this issue, such as [31]–[37]. We use the widely used global congruency test in this paper. In this section, the global congruency test is presented, and an example is given to illustrate that the underground points of the immersed tunnel are stable.

### A. GLOBAL CONGRUENCY TEST

Assuming that a control network is measured twice at different times, the coordinates obtained by the two epochs are $x_1$ and $x_2$ respectively. Their corresponding cofactor matrices and posterior variance factors are $Q_{x_1}$ and $Q_{x_2}$, $\hat{\sigma}_1^2$ and $\hat{\sigma}_2^2$. It is assumed that $x_1$ and $x_2$ are uncorrelated. If the test to check the compatibility of the estimated posterior variance factors is accepted, the displacement of the coordinates is defined as

$$d_{(x)} = x_2 - x_1 \tag{15}$$

Its cofactor matrix is

$$Q_{d_{(x)}} = Q_{x_1} + Q_{x_2} \tag{16}$$

The variance factor of $d_{(x)}$ is

$$\hat{\sigma}_{d_{(x)}}^2 = \frac{(d_{(x)})^T Q_{d_{(x)}}^+ d_{(x)}}{f_{d_{(x)}}} \tag{17}$$

where $Q_{d_{(x)}}^+$ is Moore-Penrose inverse of the cofactor matrix $Q_{d_{(x)}}$, $f_{d_{(x)}}$ is the number of independent element in $d_{(x)}$.

The total estimated variance factor is

$$\hat{\sigma}_0^2 = \frac{f_1 \hat{\sigma}_1^2 + f_2 \hat{\sigma}_2^2}{f_1 + f_2} \tag{18}$$

where $f_1$ and $f_2$ are the degrees of freedom of the two different epochs.

In order to analyze the stability of the control network, the following two hypotheses are put forward

$$H_0 : E\left(\hat{\sigma}_{d_{(x)}}^2\right) = E\left(\hat{\sigma}_0^2\right); \quad H_1 : E\left(\hat{\sigma}_{d_{(x)}}^2\right) > E\left(\hat{\sigma}_0^2\right) \tag{19}$$

The test statistic is set as

$$F = \frac{\hat{\sigma}^2_{d_{(x)}}}{\hat{\sigma}^2_0} \sim F\left(f_{d_{(x)}}, f_1 + f_2\right) \tag{20}$$

where $F\left(f_{d_{(x)}}, f_1 + f_2\right)$ is the Fisher's distribution with degrees of freedom $f_{d_{(x)}}$ and $f_1 + f_2$. If $F < F_\alpha\left(f_{d_{(x)}}, f_1 + f_2\right)$, the null hypothesis is accepted with the significance level $(\alpha)$, and the control network is stable. The control network is stable, which of course shows that our points of interest are stable. Otherwise, it indicates that there are unstable points in the network. To determine whether the points of interest are stable, the control points are divided into two groups, the stable point group M and the unstable point group U. Correspondingly, $d_{(x)}$ and $Q^+_{d_{(x)}}$ are rewritten as

$$d_{(x)} = [d_U \quad d_M]^T \tag{21}$$

$$Q^+_{d_{(x)}} = \begin{bmatrix} P_U & P_{UM} \\ P_{MU} & P_M \end{bmatrix} \tag{22}$$

The variance factor of $d_M$ is

$$\hat{\sigma}^2_{d_M} = \frac{(d_M)^T \bar{P}_M d_M}{f_{d_M}} \tag{23}$$

where $f_{d_M}$ is the dimension of $d_M$; $\bar{P}_M$ is

$$\bar{P}_M = P_M - P_{MU} P_U^{-1} P_{UM} \tag{24}$$

For the stable point group M, the test statistic is set as

$$F_M = \frac{\hat{\sigma}^2_{d_M}}{\hat{\sigma}^2_0} \sim F\left(f_{d_M}, f_1 + f_2\right) \tag{25}$$

If $F_M < F_\alpha\left(f_{d_M}, f_1 + f_2\right)$, the null hypothesis is accepted with the significance level $(\alpha)$, and the point group M is stable. This indicates that points of interest are stable.

### B. CONTROL POINTS STABILITY OF AN IMMERSED TUNNEL

In this subsection, taking the Hong Kong-Zhuhai-Macau Bridge immersed tunnel as an example, the stability of underground control points is illustrated through the analysis of the measured data. The configuration of the control network is as shown in Fig. 1b. The total station with the nominal accuracy of $0.5''$ for the angle and of $a = 1$ mm and $b = 1$ ppm for the distance was used. We select two periods of measurement data separated by 10 months. The time of the first epoch is Feb. 2015, and the time of the second epoch is Dec. 2015. The interval between the two epochs is relatively long, and no point was damaged during the period. The control points stability can be reflected by the analysis of the two epochs of data.

The network includes 8 underground points at each epoch. The point name, point location and the displacement of the coordinates are shown in Table 1. For this network, $f_1 = f_2 = 12, f_{d_{(x)}} = 12$. The significance level $\alpha$ is set to be 0.05. After analysis, $F < F_{0.05}(12, 24)$. Hence, the network is stable. No significant displacements of the control points occurred during the ten-month period. Other data of different epochs have similar results after stability analysis. The conclusion that in the horizontal direction the underground points inside the immersed tunnel have good stability can be drawn.

**TABLE 1. Point name and the displacement of the coordinates.**

| Point name | Point location | $\Delta x$ (mm) | $\Delta y$ (mm) |
|---|---|---|---|
| A1 | E1 | -1.7 | 0.1 |
| B1 | E1 | -0.6 | 0.1 |
| A2 | E5 | -0.1 | -1.5 |
| B2 | E5 | -0.6 | -1.4 |
| A3 | E9 | 3.1 | -1.5 |
| B3 | E9 | 0.5 | -0.5 |

## IV. NEW ALIGNMENT AND BREAKTHROUGH ACCURACY OPTIMIZATION STRATEGY

In this section, the new alignment and breakthrough accuracy optimization strategy for long immersed tunnels which makes use of the results of the element positioning system is presented. After the element is installed, both the positioning system and breakthrough survey can provide the position of the element. The consistency analysis between the two different positions ensures that the two kinds of results are statistically consistent. Based on this, the element position from the positioning system is taken as the constraints when the accuracy of the control network degrades to a certain degree with the increase of the number of elements installed. A joint adjustment will be conducted together with the angle and distance observations of the inside network. As the lengths of the immersed tunnels are different, the numbers of the constraints may be different.

### A. CONSISTENCY ANALYSIS METHOD

There are multiple feature points in each element. For a newly installed element, there are two different position results. One result is provided by the positioning system, denoted as $(X^d, Y^d)$. The superscript $d$ means that the coordinates are measured directly. The other is obtained by the breakthrough survey, denoted as $(X^t, Y^t)$. The superscript $t$ means that the coordinates are transferred through the control network from the surface known points. The accuracy of the results is $(m^d_x, m^d_y)$ and $(m^t_x, m^t_y)$. The coordinates are normally distributed. Bland proposed a method for consistency analysis of results obtained by different methods [38]. Based on this, a consistency analysis method is formed by adding the constraint that the mean of the differences is approximately zero. The steps of consistency analysis are:

1) Calculate the differences $(d_x, d_y)$ between the methods and their averages $\left(\bar{d}_x, \bar{d}_y\right)$.
2) Calculate the standard deviations of the differences $(s_{dx}, s_{dy})$. $s_{dx} = \sqrt{(m^d_x)^2 + (m^t_x)^2}$, $s_{dy} = \sqrt{(m^d_y)^2 + (m^t_y)^2}$.
3) 95% of the differences lie in the interval $[d_{low}, d_{up}]$. For $d_x$, $d_{low} = \bar{d}_x - 1.96 s_{dx}$, $d_{up} = \bar{d}_x + 1.96 s_{dx}$. For $d_y$, the calculation is similar.
4) Calculate the standard errors of $\bar{d}_x$ and $\bar{d}_y$. $m_{\bar{d}x} = s_{dx}/\sqrt{n}$, $m_{\bar{d}y} = s_{dy}/\sqrt{n}$, where $n$ is the size of $d_x$ and $d_y$.
5) If no less than 95% of the differences are in the interval $[d_{low}, d_{up}]$, $\left|\bar{d}_x\right| < 2m_{\bar{d}x}$, and $\left|\bar{d}_y\right| < 2m_{\bar{d}y}$, the

results of the two methods are consistent. A plot of the differences against their mean is also very informative.

### B. NEW DATA PROCESSING STRATEGY

At the initial stage of the construction of an immersed tunnel, when the number of installed elements is small, the accuracy requirement of alignment control can be met by arranging points in pairs and using the data processing method described in section 2 through measuring angles and distances. With the continuous extension of the control network, the lateral accuracy becomes lower. When the control network reaches a certain length, its accuracy will decline to the point that it no longer meets the requirement. The last point pair is denoted as the $N^{th}$ pair. The coordinates of the $N^{th}$ point pair measured by the positioning system are $(X^d, Y^d)$.

Take the coordinates $(X^d, Y^d)$ as observations. Then the observations include angles $L_\theta$, distances $L_s$, and coordinates $L_c$. In this case, the observation equation (1) becomes:

$$\begin{cases} v_\theta = A_\theta \hat{x} - l_\theta \\ v_s = A_s \hat{x} - l_s \\ v_c = A_c \hat{x} - l_c, \end{cases} \tag{26}$$

According to the steps of the outlier detection, VCE and the constraint adjustment, the new coordinates of the control network with higher accuracy can be obtained. Update the control network coordinates. Once an element has been installed, the positioning system will be removed soon. So we select specific point pairs with good stability and relatively far from the portal as constraints, continue to install new elements, and extend the control network. The angle and distance observations are processed together with the coordinate constraints. Until the control network no longer meets the accuracy requirements of alignment control, then the new coordinates $(X^d, Y^d)$ are taken as additional constraints to obtain the coordinates of the control network with higher accuracy. Update the control network coordinates and select new extra special points to add to the constraint set, continue to install new elements, and extend the control network. The angle and distance observations are processed together with the coordinate constraints. Repeat the above procedures until the tunnel finally breaks through.

The steps of the new data processing strategy are as follows:

1) When the first few elements are installed, angles and distances are measured and the constrained adjustment as described in section 2 is performed. The constraint set is empty.
2) When the accuracy of the end point decays to a certain degree, take the coordinate of the feature point of the newly installed element as the additional observation, and perform a joint adjustment with the angle and distance observations of the inside network, and the constraint set (if not empty). At this time, the network contains $N$ point pairs.
3) Update the coordinates of the network. Add the coordinates of the $(N-1)^{th}$ point pair to the constraint set.
4) Continue to install elements. Perform the joint adjustment with the angle and distance observations of the inside network, and the constrained set.
5) When the accuracy of the weakest point of the network decays to a certain degree, return to 2). Repeat this process until the tunnel breaks through.

## V. NUMERICAL RESULTS AND DISCUSSION

To investigate the performance of the new strategy for alignment and breakthrough accuracy optimization of the immersed tunnel, the results of simulation studies and an experimental traverse network are presented. All the data were processed by a self-written program.

### A. SIMULATIONS

A straight immersed tunnel that is constructed simultaneously from two opposite directions is considered (Fig. 3). The longest immersed tunnel built or under construction in the world is 17.6 km [22]. In this section, the length of the simulated immersed tunnel is set to be 20 km. The immersed tunnel consists of 112 elements, each about 180 m long. When the breakthrough point is in the middle of the tunnel, it is most conducive to the breakthrough survey [39]. So the breakthrough plane is set to be in the middle of the tunnel. The uncertainty of the tunnel alignment control shall not be more than $\pm 35$ mm. The required breakthrough accuracy is $\pm 35$ mm. The breakthrough point is located in the middle of the tunnel, and both directions have the same measurement requirements. So, we take the survey network on one side as an example for analysis. The lateral positioning error of the weakest point of the network should not be greater than $\pm 24.7$ mm.

The traverse network is designed inside the tunnel (Fig. 4). Two points of the same mileage are called a point pair. Even if the point pairs are arranged every four elements in the immersed tunnel, i.e., the distance between them is 720 m, it still has good visibility. The prior accuracy of the angle and distance observation is $\pm 1''$ and $\pm 1$ mm $+$ 0.6 ppm. The accuracy analysis was carried out when the distance between point pairs is 560 m and 720 m. 100,000 simulations were conducted for each network. The lateral accuracy of the points is shown in Fig. 5. As can be seen, when the total length of the network is constant, the longer the length of the side is, the higher the accuracy is. But neither of the two networks can meet the accuracy requirement.

In the following analysis, a point pair is arranged every four elements, and the distance between the point pairs is about 720 m. The traverse network contains 14 point pairs (Fig. 4). If the strategy proposed in this paper is adopted, the alignment control process of the immersed tunnel is as follows:

1) With the continuous installation of elements, the traverse network is gradually extended. According to the results in Fig. 5 and the red line in Fig. 6a, if the control network extends to the $14^{th}$ point pair, the

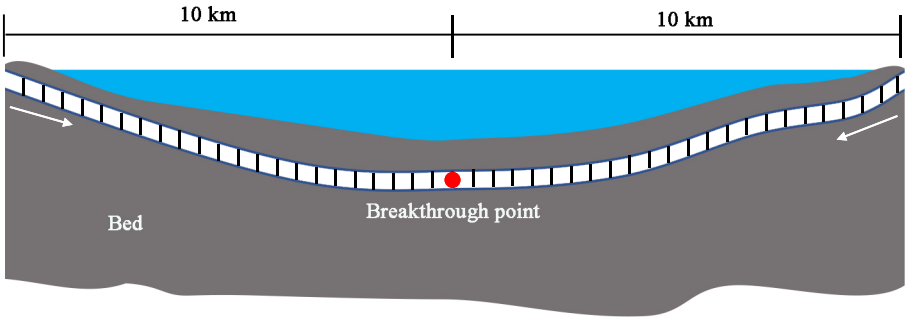


**FIGURE 3.** An immersed tunnel constructed simultaneously from two opposite directions.

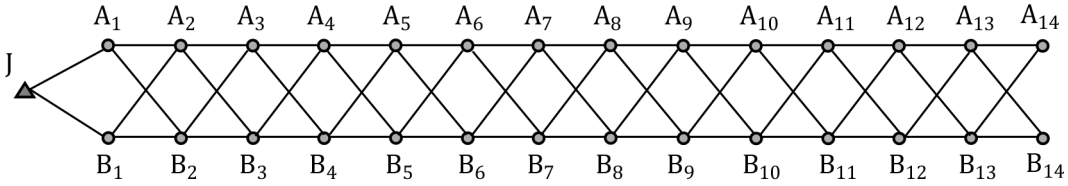


**FIGURE 4.** Ten kilometers long traverse network with the leg length of 720 m and 14 point pairs.

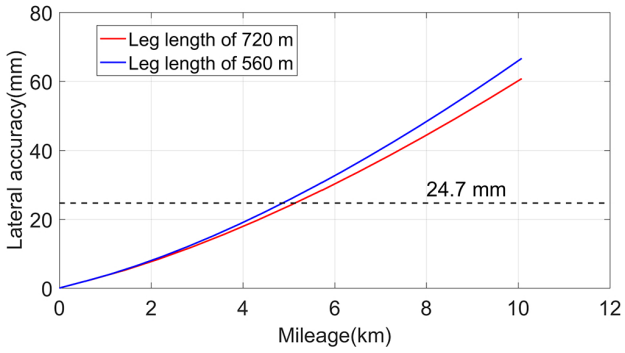


**FIGURE 5.** The absolute value of accuracy of the traverse network with the leg length of 720 mand 560 m.

lateral accuracy of the weakest point is 60.8 mm. The lateral accuracy of the $6^{th}$ point pair has decayed to 19.7 mm. Therefore, it is necessary to take the coordinates of point pair $A_6(B_6)$ obtained by the element positioning system as the observations and perform a joint adjustment with the angles and the distances. The coordinate accuracy provided by the positioning system is $m_x = 30$ mm and $m_y = 30$ mm. After data processing, the lateral accuracy of point pair $A_5(B_5)$ is increased from 15.6 mm to 11.5 mm (Fig. 6a). Then the coordinates of point pair $A_5(B_5)$ are added to the constraint set.

2) Continue to install the elements and extend the control network. According to the red line in Fig. 6b, if the control network extends to the $14^{th}$ point pair, the lateral accuracy of the weakest point is 41.2 mm. The lateral accuracy of the $9^{th}$ point pair has decayed to 18.7 mm. Take the coordinates of point pair $A_9(B_9)$ obtained by the element positioning system as the observations and perform a joint adjustment with the angles, the distances, and the coordinates of point pair $A_5(B_5)$. After data processing, the lateral accuracy of point pair $A_5(B_5)$ and $A_8(B_8)$ is increased from 7.2 mm and 15.1 mm to 4.5 mm and 9.7 mm (Fig. 6b). Then the coordinates of $A_8(B_8)$ are added to the constraint set.

3) Continue to install the elements and extend the control network. According to the red line in Fig. 6c, if the control network extends to the $14^{th}$ point pair, the lateral accuracy of the weakest point is 25.5 mm. The lateral accuracy of the $13^{th}$ point pair is 21.2 mm. Take the coordinates of point pair $A_{13}(B_{13})$ obtained by the element positioning system as the observations and perform a joint adjustment with the angles, the distances, and the constraint set. After data processing, the lateral accuracy of point pair $A_5(B_5)$, $A_8(B_8)$ and $A_{12}(B_{12})$ increases from 2.9 mm, 5.8 mm and 17.4 mm to 2.0 mm, 3.5 mm and 11.0 mm (Fig. 6c). Then the coordinates of $A_{12}(B_{12})$ are added to the constraint set.

4) Continue to install the elements and extend the control network. Until the last point pair of the control network, its lateral accuracy is 11.8 mm, which still meets the accuracy requirement. The lateral accuracy of the whole traverse network is shown as the blue line in Fig. 6c.

The accuracy of the 10 km traverse network with different number of constrained point pairs is shown in Fig. 7. It can be seen that the accuracy of the whole traverse network is significantly improved with each additional point pair coordinates as the constraints. From the starting point to the constraint point pair, the accuracy of the control network changes slowly with the increase of the mileage, and the accuracy of the subsequent control network decreases rapidly. Limited by the elongated shape of the immersed tunnels, the network was established in the form of the open-ended traverses. This type of network is the worst from the point of view of the

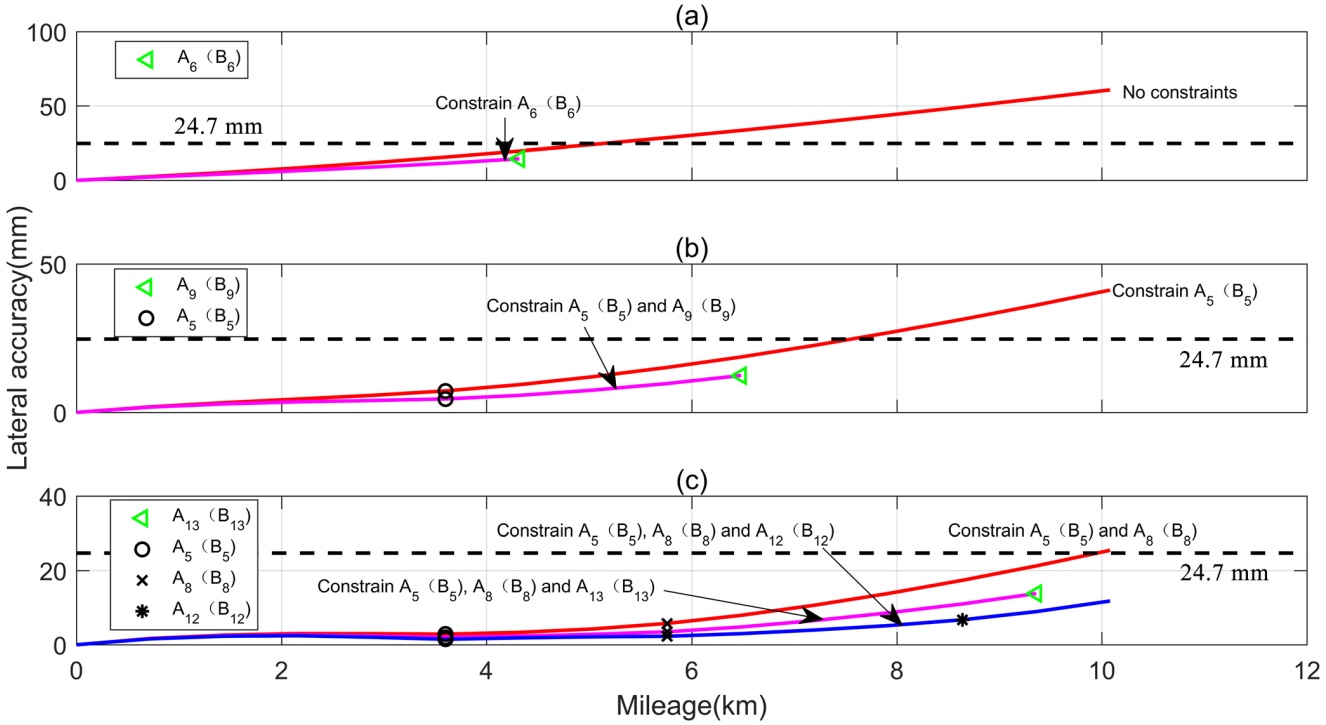


**FIGURE 6.** The absolute value of accuracy of the traverse network with different length when different number of point pairs are constrained. The ordinate scales of the three sub-figures are different. The horizontal dashed lines are the accuracy requirement, 24.7 mm.

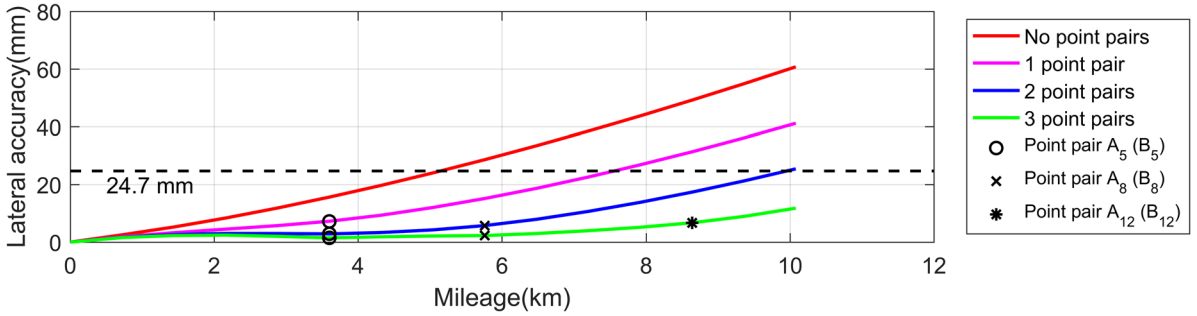


**FIGURE 7.** The absolute value of accuracy of the traverse network when coordinates of different number of point pairs are constrained.

error propagation. In comparison with angles and distances, the coordinates provided by the positioning system are independent observations. The coordinate accuracy is independent of the length of the tunnel. As the constraints, point pair coordinates can effectively reduce the propagation and accumulation of the angle errors. This is why the new strategy works. When the construction length of the immersed tunnel in one direction is less than 5 km, the measurement can be carried out only with the traverse network. If the construction length exceeds 5 km, constraints are required. The longer the construction length, the more point pairs are required as constraints.

In tunneling surveys, the common methods to improve the measurement accuracy are to add the gyro azimuth observations and to increase the complexity of the network. For comparison purposes, we analyzed the accuracy of four schemes through simulations, each of which was simulated 100,000 times. The four schemes are shown in Table 2.

**TABLE 2.** Four schemes of accuracy analysis for the alignment control.

| Scheme | Control network | Observation type | Data processing method |
|---|---|---|---|
| 1 | Traverse network | Angle and distance | Current method |
| 2 | Traverse network | Angle, distance and azimuth | Current method |
| 3 | Duo-linear joint chain | Angle and distance | Current method |
| 4 | Traverse network | Angle and distance | New method |

In scheme 2, the azimuth is measured every 2 km. The azimuths of 4 sides were measured. The sides are $A_3 \rightarrow B_4$, $A_6 \rightarrow B_7$, $A_9 \rightarrow B_{10}$, $A_{12} \rightarrow B_{13}$. The prior accuracy of the azimuth observations is $\pm 3.5''$. In scheme 3, the duo-linear joint chain, which was designed for the alignment control of Hong Kong-Macau-Zhuhai Bridge immersed tunnel, is shown in Fig. 2c.

The lateral accuracy of the 4 schemes are shown in Fig. 8. The accuracy is improved by adding the gyro azimuths and increasing the complexity of the control network. Compared

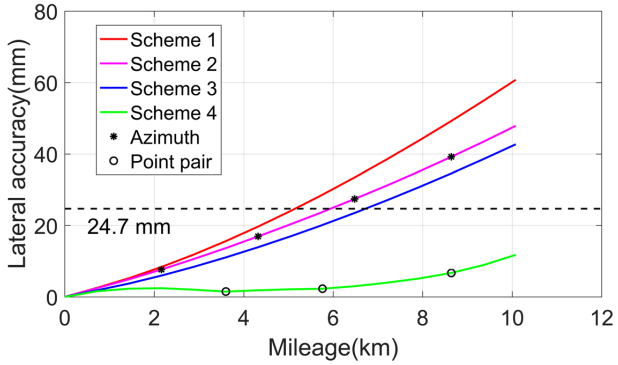


**FIGURE 8.** The absolute accuracy of different schemes for the alignment control of the 10 km immersed tunnel.

with scheme 1, the lateral accuracy of the weakest point is improved by 22.2% and 29.7% respectively. The results are consistent with the results in literature [18] and [19]. But the scheme 1, 2 and 3 cannot meet the accuracy requirement. If the traditional alignment control strategy is adopted, it is necessary to further increase the number of gyro azimuths or increase the complexity of the network.

However, using the new alignment control strategy for long immersed tunnels proposed in this paper, only the coordinates of three point pairs provided by the positioning system are used as the constraints, and the lateral accuracy of the weakest point is as high as 11.8 mm. According to the curve of lateral accuracy, the accuracy decays slowly in the interval from the starting point of the control network to the last constrained point pair. Even if the tunnel length continues to increase, as long as the number of the constrained point pairs is increased, the new strategy can still effectively control the tunnel alignment.

### B. EXPERIMENT

The experiment was carried out in Zhuhai, Guangdong Province, China (longitude: E 113.6°; latitude: N 22.1°).

**TABLE 3.** Basic information of the experimental traverse networks.

| Property | Left network | Right network |
|---|---|---|
| Total length | 5.8 km | 1.0 km |
| Length of side | 720 m | 180 m |
| Number of angles | 67 | 35 |
| Number of distances | 34 | 18 |

A GPS network and two traverse networks were designed on the ground to simulate the breakthrough survey of an immersed tunnel. The network is shown in Fig. 9. The triangle symbol represents the surface point; the circular symbol indicates the ''underground'' point. In order to distinguish it from the point name in Fig. 4, the subscript of the point name of the traverse network in Fig. 9 is not a continuous number, but the No. of the analog element where it is located. $A_{29}$ is the breakthrough point. The underground points were laid along a road. The surface points and the breakthrough point were measured using Trimble R7 receivers. Leica TS30 was used to measure the angles and distances of the traverse networks. The basic information of the traverse networks is shown in Table 3.

The GPS data were processed as follows:

1) The GPS data of $W_1$ and $E_1$ together with the data of IGS (International GNSS Service) stations, wuhn, tnml and cusv, were processed with the GAMIT/GLOBK software. The baselines and the earth frame coordinates of $W_1$ and $E_1$ were obtained.
2) The experimental coordinate system (ECS) was established through Gauss-Krüger projection. And the length and azimuth of the side $W_1 \rightarrow E_1$ were calculated.
3) Taking this length and azimuth as known data, the baselines were adjusted to obtain the ECS coordinates of the surface points and the breakthrough point.

The angle and distance observations of the left and right network were processed in the method described in Section II.

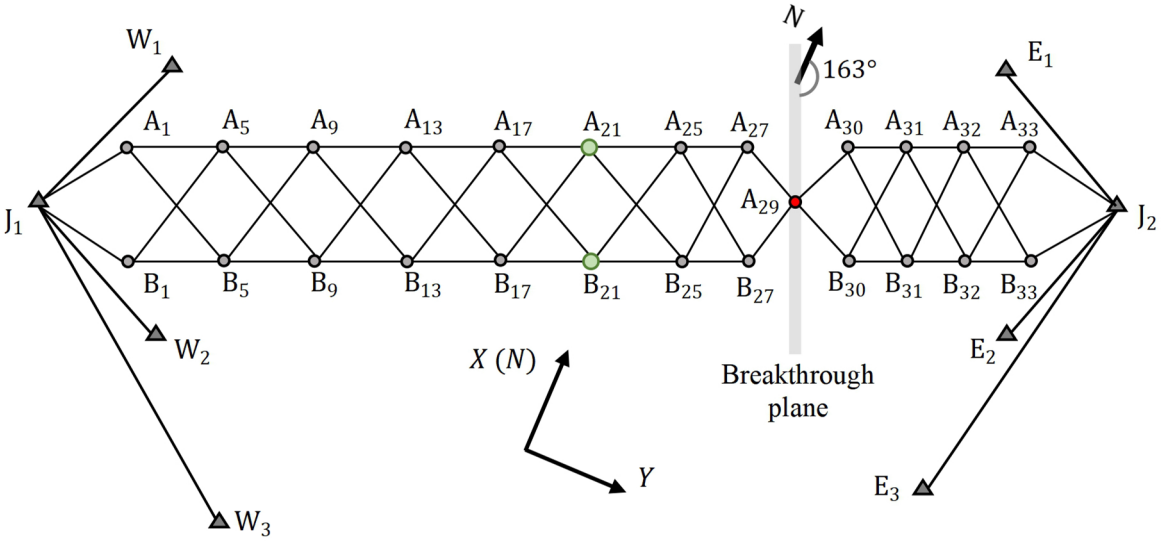


**FIGURE 9.** The experimental control network.

**TABLE 4. The coordinate differences of the breakthrough point and breakthrough errors in the experiment.**

| Diff. | Current data processing method | | New strategy | |
|---|---|---|---|---|
| | $\Delta X$ (mm) | $\Delta Y$ (mm) | $\Delta X$ (mm) | $\Delta Y$ (mm) |
| Left - GPS | 57.1 | -24.9 | -20.8 | 1.8 |
| Right - GPS | -6.0 | 2.3 | -6.0 | 2.3 |
| Right - Left | -63.1 | 27.2 | 14.8 | 0.5 |
| Breakthrough error (mm) | | | | |
| Lateral | -52.4 | | 14.3 | |
| Longitudinal | 7.6 | | 4.8 | |

There are three different ECS coordinates for the breakthrough point, which are measured by GPS, measured by the left network, and measured by the right network. Besides, the new strategy was adopted to process the observations of the left network. Referring to the results in the previous subsection, we take the coordinates of the sixth point pair, $A_{21}$ and $B_{21}$, as the extra observations, and adjust them together with the angle and distance observations to obtain a more accurate network. The coordinates of $A_{21}$ and $B_{21}$ were obtained through a duo-linear joint chain as shown in Fig. 2c. The results of both methods are shown in Table 4. If the coordinate of $A_{29}$ measured by GPS is taken as the ''true'' value, the ''true'' error of the coordinate of $A_{29}$ visually represents the accuracy of the network. Due to the accumulation of the angle errors, the accuracy of the traverse network decreases with the increase of its length. The total length of the network on the right side is smaller, so the true errors obtained in the current data processing method is also smaller. After the new strategy is used to process the same observations, the true errors of the left network is greatly reduced. Moreover, the breakthrough errors, especially the lateral error, have been greatly reduced. The absolute value of the lateral breakthrough error decreased from 52.4 mm to 14.3 mm. This indicates that the new strategy in this paper significantly optimizes the accuracy of the control network, and it has remarkable effect on the optimization of the immersed tunnel breakthrough accuracy.

## VI. CONCLUSION

In recent years, immersed tunnels have developed rapidly around the world, and longer immersed tunnels have appeared. Currently, the longest immersed tunnel under construction has reached 17 km. The immersed tunnel has unique engineering characteristics, construction environments and higher alignment and breakthrough accuracy requirements. In order to maintain good water tightness and structural safety of the tunnel, the elements must be accurately connected. In order to improve the accuracy of the alignment and the breakthrough, a new control strategy is proposed. Firstly, the stability analysis is conducted to illustrate that the underground points of the immersed tunnel are stable. Then, through the consistency analysis, the results of the element positioning system and the results of the control network are verified to be consistent. Finally, the results of the element positioning system are used as constraints to improve the accuracy of the control network. A 20 km-long immersed tunnel was simulated and an experiment was conducted to demonstrate the performance of the proposed strategy. Following the new strategy, it can be guaranteed that the lateral accuracy of the alignment control and breakthrough of the immersed tunnel are better than 20 mm. As long as new coordinates are continuously added to the constraint set, the accuracy of the control network can always be maintained at a high level. The new strategy can be introduced as a reliable method that provides accurate results for the alignment control and the breakthrough of the immersed tunnels under construction and planning.

## REFERENCES


[1] S. C. Stiros, ''Alignment and breakthrough errors in tunneling,'' *Tunnelling Underground Space Technol.*, vol. 24, no. 2, pp. 236–244, Mar. 2009.

[2] A. Chrzanowski, ''Optimization of the breakthrough accuracy in tunneling surveys,'' *Can. Surveyor*, vol. 35, no. 1, pp. 5–16, Mar. 1981.

[3] A. Johnston, ''Lateral refraction in tunnels,'' *Surv. Rev.*, vol. 31, no. 242, pp. 201–220, Oct. 1991.

[4] A. Chrzanowski, W. T. Greening, J. Grodecki, and J. Robbins, ''Design of geodetic control for large tunneling projects,'' in *Proc. Annu. Publication Tunneling Assoc. Canada*. Richmond, VA, USA: Tunnelling Association of Canada, 1993, pp. 1–11.

[5] N. Korritke, ''Application of high precision gyrotheodolites in tunnelling,'' in *Proc. FIG Symp. Surveying Large Bridge Tunnel Projects*, Copenhagen, Denmark, 1997, pp. 195–213.

[6] M. Schafer and G. Weithe, ''Survey solution on the construction sites North Downs Tunnel and Medway Crossing Bridge–HighSpeed-railway from London to the Eurotunnel,'' in *Proc. Geodesy Geotechn. Struct. Eng.*, Berlin, Germany, 2002, pp. 156–165.

[7] N. Korittke, ''Influence of Horizontal refraction on traverse measurements in tunnels with small diameter,'' in *Proc. 2nd Int. Workshop Accel. Alignment*, Hamburg, Germany, Sep. 1990, pp. 315–331.

[8] A. Johnston, ''Tunnel alignment and lateral refraction,'' *Tunnels Tunnelling Int.*, vol. 30, no. 3, pp. 58–60, 1998.

[9] J. Velasco-Gómez, J. F. Prieto, I. Molina, T. Herrero, J. Fábrega, and E. Pérez-Martín, ''Use of the gyrotheodolite in underground networks of long high-speed railway tunnels,'' *Surv. Rev.*, vol. 48, no. 350, pp. 329–337, Sep. 2016.

[10] J. Velasco, J. Prieto, T. Herrero, and J. Fabrega, ''Geodetic network design and strategies followed for drilling a 25 km tunnel for high-speed railway in Spain,'' in *Proc. FIG Congr.*, Sydney, NSW, Australia, 2010, pp. 11–15.

[11] I. Lewén, ''Use of gyrotheodolitein underground control network,'' Ph.D. dissertation, School Archit. Built Environ., KTH, Stockholm, Sweden, 2006.

[12] H. Ingensand, ''Concepts and solutions to overcome the refraction problem in terrestrial precision measurement,'' *Geodesy Cartography*, vol. 34, no. 2, pp. 61–65, Jun. 2008.

[13] H. Ingensand, A. Ryf, and R. Stengele, ''The gotthard tunnel—A challenge for geodesy and geotechnics,'' in *Proc. Geodesy Geotechn. Struct. Eng.*, ETH, Zurich, Switzerland, Apr. 1998, pp. 20–22.

[14] F. Brunner and E. Grillmayer, ''On the temperature dependence of gyroscopic measurements using the GYROMAT 2000,'' in *Proc. 22nd FIG Int. Congr.*, Washington, DC, USA, 2002, pp. 1–11.

[15] J. Martusewicz, ''Optimal location of extra gyroscopic azimuth in underground traverses,'' *J. Surveying Eng.*, vol. 119, no. 4, pp. 137–146, Nov. 1993.

[16] H. Hu, J. Gao, J. Sun, and Z. Li, ''Gyro side self adaptive weighting rigorous adjustment model based on configuration structure,'' *J. China coal Soc.*, vol. 38, no. 10, pp. 1786–1791, 2013.

[17] J. Ma, Z. Yang, Z. Shi, C. Liu, H. Yin, and X. Zhang, ''Adjustment options for a survey network with magnetic levitation gyro data in an immersed under-sea tunnel,'' *Surv. Rev.*, vol. 51, no. 367, pp. 373–386, Jul. 2019.

[18] S. Huang, G. Li, X. Wang, and W. Zhang, ''Geodetic network design and data processing for Hong Kong–Zhuhai–Macau link immersed tunnel,'' *Surv. Rev.*, vol. 51, no. 365, pp. 114–122, Mar. 2019.

[19] G. Li and S. Huang, ''Control survey for a 6.7 km immersed tunnel in Chinese Lingding ocean,'' *J. Appl. Geodesy*, vol. 13, no. 3, pp. 257–265, Jul. 2019.

[20] M. A. Alizadeh-Khameneh and J. V. Andersson, ''Geodetic network design in tunnel surveys,'' *J. Surveying Eng.*, vol. 146, no. 4, Nov. 2020, Art. no. 06020003.

[21] R. Haag, F. Braker, and R. Stengele, "A 57km long railway tunnel through the Swiss Alps and its planned survey," in *Proc. 21st FIG Int. Congr.*, Brighton, U.K., 1998, pp. 22–32.
[22] B. Huck, A. Jensen, and A. Almholt, "The Fehmarnbelt positioning system for a mega construction site," in *Proc. Eur. Navigat. Conf. (ENC)*, Vienna, Austrian, 2013, pp. 1–5.
[23] C. Fang and J. Zhao, "Development of an integrated measurement system used for immersed-tube installation in Guangzhou Zhoutouzui project," *China Harbour Eng.*, vol. 194, no. 4, pp. 21–25, 2014.
[24] W. Grafarend, "Optimization of geodetic networks," *Can. Surveyor*, vol. 28, no. 5, pp. 716–723, 1974.
[25] W. Baarda, "A testing procedure for use in geodetic networks," Netherlands Geodetic Commission, Publications Geodesy, Delft, The Netherlands, New Ser. 2, no. 5, 1968.
[26] J. Kok, "On data snooping and multiple outlier testing," U.S. Dept. Commerce, Nat. Ocean. Atmos. Admin., Charting Geodetic Services, Nat. Ocean Service, Silver Spring, MD, USA, NOAA Tech. Rep. NOS NGS 30, 1984, vol. 30.
[27] B. Li, Y. Shen, and L. Lou, "Efficient estimation of variance and covariance components: A case study for GPS stochastic model evaluation," *IEEE Trans. Geosci. Remote Sens.*, vol. 49, no. 1, pp. 203–210, Jan. 2011.
[28] K. Koch, *Parameter Estimation and Hypothesis Testing in Linear Models*. Berlin, Germany: Springer, 2013, pp. 153–181.
[29] B. Li, "Surveying network design and adjustment for ballastless track HSR: Case study with the first HSR in China," *J. Surveying Eng.*, vol. 142, no. 3, Aug. 2016, Art. no. 04015015.
[30] E. Grafarend, A. Kleusberg, and B. Schaffrin, "An introduction to the variance-covariance component estimation of Helmert type," *Zeitschrift für Vermessungswesen*, vol. 105, no. 4, pp. 161–180, 1980.
[31] J. van Mierlo, "A testing procedure for analysing geodetic deformation measurements," in *Proc. 2nd Int. Symp. Deformation Meas. Geodetic Methods*, Stuttgart, Germany, 1978, pp. 321–353.
[32] C. Fraser and L. Gruendig, "The analysis of photogrammetric deformation measurements on Turtle Mountain," in *Proc. Eng. Surveys Conf.*, vol. 6. Washington, DC, USA: International Federation of Surveyors, Commission, 1984.
[33] M. A. R. Cooper, *Control Surveys in Civil Engineering*. New York, NY, USA: W. G. Nichols, Inc., 1987, pp. 331–345.
[34] Y. Chen, "Analysis of deformation surveys—A generalized method," Ph.D. dissertation, Dept. Geodesy Geomatics Eng., Univ. New Brunswick, Fredericton, NB, Canada, 1983.
[35] Y. Q. Chen, A. Chrzanowski, and J. M. Secord, "A strategy for the analysis of the stability of reference points in deformation surveys," *CISM J.*, vol. 44, no. 2, pp. 141–149, Jul. 1990.
[36] Z. Wiśniewski, "Estimation of parameters in a split functional model of geodetic observations ($M_{split}$ estimation)," *J. Geodesy*, vol. 83, no. 2, pp. 105–120, Feb. 2009.
[37] K. Nowel and W. Kamiński, "Robust estimation of deformation from observation differences for free control networks," *J. Geodesy*, vol. 88, no. 8, pp. 749–764, Aug. 2014.
[38] J. Bland and D. Altman, "Statistical methods for assessing agreement between two methods of clinical measurement," *Lancet*, vol. 1, no. 8476, pp. 10–307, 1986.
[39] X. Wang, S. Huang, G. Li, C. Li, and W. Zhang, "Theoretical analysis of the influence of plane control network on lateral breakthrough error of long immersed tunnel," *J. Appl. Geodesy*, vol. 14, no. 3, pp. 241–251, Jul. 2020.

**GUANQING LI** was born in Dongming, Shandong, China, in 1990. He received the B.S. degree in geomatics and the M.S. degree in geodesy and geomatics from Wuhan University, in 2013 and 2016, respectively, where he is currently pursuing the Ph.D. degree in geodesy and geomatics.

From 2013 to 2017, he was a Survey Technical Consultant with the Project Management Department for Island & Tunnel Project of Hong Kong-Zhuhai-Macao Bridge. From 2019 to 2020, he was a Visiting Student with the Institute for Geodesy and Geoinformation, Bonn University, Germany. His research interests include precise engineering surveying, data processing, and deformation monitoring.

**SHENGXIANG HUANG** was born in Jiangxi, China, in 1964. He received the B.S. and M.S. degrees from the Wuhan Technical University of Surveying and Mapping, in 1986 and 1993, respectively, and the Ph.D. degree in geodesy and geomatics from Wuhan University, in 2001.

From 1992 to 1996, he was a Lecturer with Wuhan Technical University. From 1996 to 2000, he was an Assistant Professor with Wuhan Technical University. Since 2000, he has been a Professor with Wuhan University. His research interests include deformation monitoring and disaster early warning, GNSS application, and precise engineering surveying.

**XINPENG WANG** was born in Nanyang, Henan, China in 1982. He received the B.S. degree in surveying and mapping engineering from Henan Polytechnic University, in 2006, the M.S. degree in geodesy and surveying engineering from Hefei University of Technology, in 2012, and the Ph.D. degree in geodesy and surveying engineering from Wuhan University, in 2020.

Since 2020, he has been a Lecturer with the Department of Surveying and Mapping Engineering, College of Mining, Guizhou University. His research interests include precision engineering measurement, deformation monitoring, and disaster early warning.

**CHENFENG LI** was born in Jiangxi, in 1990. He received the M.S. degree in geodesy and surveying engineering from Jiangxi Polytechnic University, in 2015, and the Ph.D. degree in geodesy and surveying engineering from Wuhan University, China, in 2020. His research interests include crustal deformation and precise integrated positioning.

**WEN ZHANG** was born in Hubei, China, in 1988. He received the B.S. degree in geomatics, and the M.S. and Ph.D. degrees in geodesy and geomatics from Wuhan University, in 2011, 2013, and 2020, respectively. His research interests include precise engineering surveying, and deformation monitoring analysis and disaster forecast.